CrossMark

Effect of deposition time on sputtered ZnO thin films and their gas sensing application

Sonik Bhatia[1] · Neha Verma[1,2] · Munish Aggarwal[3]

Abstract

Nowadays, advanced industrialization and population growth have led to increasing the environmental related issues. This paper reports the effect of deposition time on ZnO films deposited on to the glass substrate by using rf magnetron sputtering technique and their further use for gas sensing applications. Herein, deposition time is considered to be changed from 300 s, 800 s (S1, S2). The thickness of deposited films lies in the range of 130–180 nm. The synthesized films were characterized by various techniques in terms of structural, morphological, optical and gas sensing properties. The typical crystal size of ZnO films was found to be in the range of 15–27 nm. FESEM analysis revealed the growth of nanospheres was lies in the range of 80–120 nm. Fourier transform infrared spectroscopy confirmed the ZnO bonding located at a wavelength of 430 cm^{-1}. The average optical transmittance of the film was about 90–95% in the visible range. The optical band gap of ZnO films was decreased from 3.31 to 3.29 eV. The detailed characterization study showed 800 s is an optimum deposition time for good optoelectronic properties. For gas sensing application, highest sensitivity was obtained at operating temperature of 205 °C. Prepared films have a quick response and fast recovery time in the range of 128 s and 163 s respectively. These response and recovery time characteristics were explained by valence ion mechanism.

1 Introduction

In the recent years, increasing the demand for advanced technology is an essential issue to create smart and functional materials necessitated the search of attractive and inexpensive transparent conducting oxide (TCO). As one such TCO is ZnO, it has been extensively studied as a member of II–VI group semiconductor having wide direct band gap 3.37 eV [1] and high exaction binding energy of 60 meV at room temperature compared with the wide bandgap of other materials such as GaN (3.4 eV) and binding energy 21 meV which is approximately 2.9 times less than the binding energy of ZnO. It can be combined with GaN for LED applications. ZnO is an n-type semiconductor has unique electrical, optical and luminescent properties. It holds a great deal of promise for developing advanced technology liquid crystal display, light emitting diode [2], optical waveguides, solar cells [3]. Due to these attractive properties, TCO vapor has some advantages for toxic and hazardous gases. It is also useful for oxygen gas sensors due to its mechanism based on oxygen vacancies. As it is transparent material absorptive in the UV region and transparent in visible range so it can be used as UV detector. Copper oxide NWs are multifunctional materials and it has also many optoelectronic applications [4].

Including physical and chemical routes, ZnO has been synthesized by a variety of techniques such as chemical deposition [5], spray pyrolysis [6], sol–gel with spin coating [7], dip coating [8], simple heat treatment method [9] and rf magnetron sputtering [10]. Among these techniques, rf magnetron sputtering has more advantages over the others in term of cost, simplicity in process control, it can deposit uniform films over a large area. One of the important advantages of the sputtering technique is that some of the depositing parameters such as base pressure, substrate temperature, rf power, deposition time, the distance between target and substrate can be easily controlled. These parameters play a vital role to improve the sensitivity for gas sensing applications.

✉ Sonik Bhatia
    sonikbhatiaphysics@gmail.com

1   PG Department of Physics, Kanya Maha Vidyalaya, Jalandhar 144004, India

2   IKG Punjab Technical University, Kapurthala 144601, India

3   Lyallpur Khalsa College of Engineering, Jalandhar 144001, India

Saikia et al. [11] revealed that sensing behavior of ZnO nanoparticles was better for H_2S as compared to CO, H_2, Cl_2. The literature reported that Rf magnetron sputtering technique is performed by varying different parameters. Nafarizal reported the external parameters plays an important role to optimize the properties of ZnO films for the gas sensing applications [12]. Dwivedi et al. reported that the maximum sensitivity towards CO is found to be 52%. These samples were annealed at 400 °C temperature to find better gas sensitivity [13]. Peng et al. [14] observed that low sputtering power (100 W) and substrate temperature 300–400 °C are most suitable experimental conditions for the growth of ZnO films. Ndong et al. [15] found that the best quality of ZnO films has been grown on Silicon substrate at the target to substrate distance is 7 cm. Becerril et al. [16] achieved the band gap of the film increases with Al doping. Hoon et al. [17] observed that with an increase in film thickness, the grain size of film increases in dc magnetron sputtering and films have a high optical transmittance in the range of 60–90%. The morphology, particle size, surface to volume ratio, the remarkable electronic conductivity of the metal oxide semiconductor strongly influenced on gas sensing properties [18]. Fang et al. reported that one-dimensional inorganic semiconductors are new carriers for nanosensors [19].

To date, researchers are trying their best efforts to find the gas response at room temperature. Till now it has found that this activity cannot be performed at room temperature. In the present investigation, deposited films were analyzed at 205 °C for gas sensing properties. Quick response and fast recovery time is the cause of controlled parameters. To obtain the better gas sensing property, researchers are adopting different approaches such as annealing temperature, varying deposition time, substrate, doping elements and synthesis techniques [20–24]. It has been reported that the gas sensing parameters do not only influence on the surface to volume ratio and particle size but also interconnection present between metal oxide nanoparticles [25]. An effect of ZnO film on the morphological, structural, optical and gas sensing properties have been studied by using XRD, FESEM, UV–Vis, FTIR, PL spectroscopy and gas sensing properties.

2 Experimental details

A thin film of ZnO has been prepared by rf magnetron sputtering method on to the glass substrate at room temperature, prior to the deposition, the substrate was cleaned with distilled water, isopropyl alcohol and methanol in an ultrasonic cleaner for 10 min, dried it with nitrogen gas. Sputtering system (Anelva SPF-332H sputtering system) has ZnO target (99.99%) pure of 2-in. diameter

was sputtered in an argon atmosphere for about 200 s to remove the surface layer of the target before deposition of the film. Magnetron sputtering was carried out in argon gas by supplying rf power at a frequency of 13.56 MHz, the base pressure in the chamber prior to the deposition was maintained at 5×10^{-6} Torr controlled by a Pirani gauge, distance between target and substrate is 7.5 cm. The rf power during the growth was kept constant at 100 W. This deposition was done under an argon gas flow of 200 sccm. After the deposition process, the sample is annealed at 500 °C under N_2 for 1 h. Different thickness of ZnO films has been deposited by varying the deposition time of 300 s and 800 s (Fig. 1).

2.1 Gas sensing property

The variation in film thickness is one of the crucial factors for the application of the transparent film. ZnO films with different thickness have been deposited by varying the deposition time (300 s, 800 s) and keeping all other parameters constant. The thickness of the deposited film is measured with Profilometer which lies in the range of 130–180 nm [26, 27]. Table 1 showed that film with less deposition time has low thickness. This contributes to high transparency and reduction in resistivity.

Figure 2 shows a static gas sensing set up is used to study the gas sensing properties. The response of an active layer is measured as $S = R_a/R_g$. In order to get sensing properties, films were annealed at higher temperature. The process of annealing in the air creates more oxygen vacancies on the surface of the film.
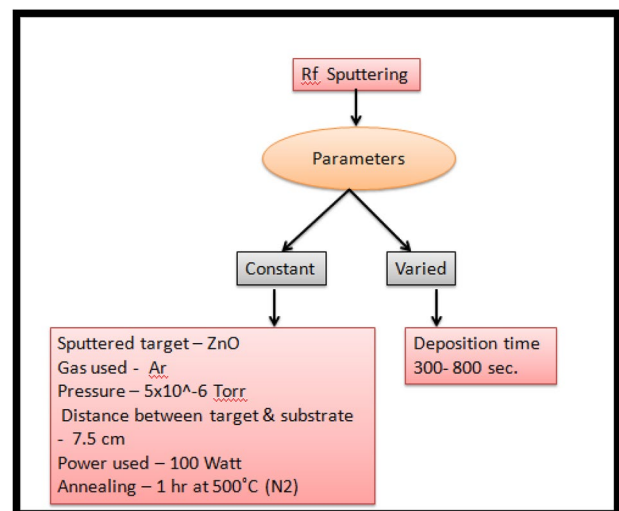

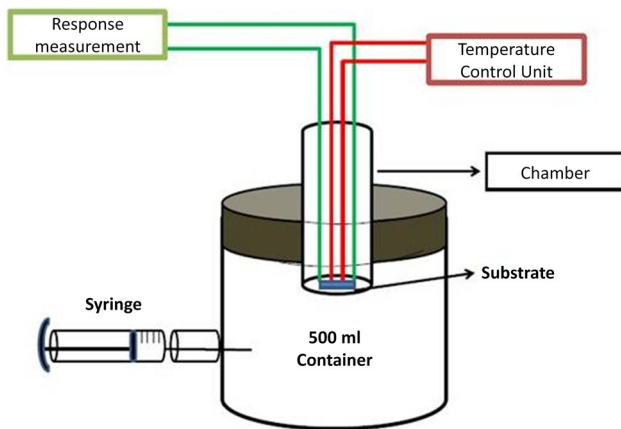**Fig. 1** Systematic scheme for rf magnetron sputtering technique

Fig. 2 Static gas sensing set up for gas sensing applications

Fig. 3 XRD spectra of ZnO films for different deposition time (300 s, 800 s) respectively

3 Results and discussion

3.1 Structural, morphological and optical properties of ZnO films

Variation in deposition time has influenced on the quality of ZnO films prepared by rf sputtering technique. To examine crystal phase and crystallinity, the prepared films were characterized by X-ray diffractometer (xpert pro with CuKα, nickel metal as β filter) in the scan range from 25° to 80°. Figure 3 shows the XRD profiles of ZnO films with the deposition time of 300 s and 800 s. XRD spectra show sharp and most intense peaks which indicate that the prepared films are well crystalline [9, 28]. A single most prominent peak appeared at a 2θ angle of 34.7° corresponds to an increase in crystal size. The increase in deposition time leads to superior diffraction peaks which show an increase in crystal size. XRD spectra represent the peak intensity of (002) peak increases and an additional peak of (202) is inserted at 74.57° which indicates the films are nanocrystalline in nature. The shift in the position of (002) plane towards the left angle may be attributed to the better crystallinity. This shows the variation in lattice parameters which reveals an importance of lattice space distribution of Zn ions which is responsible for the optoelectronic application.
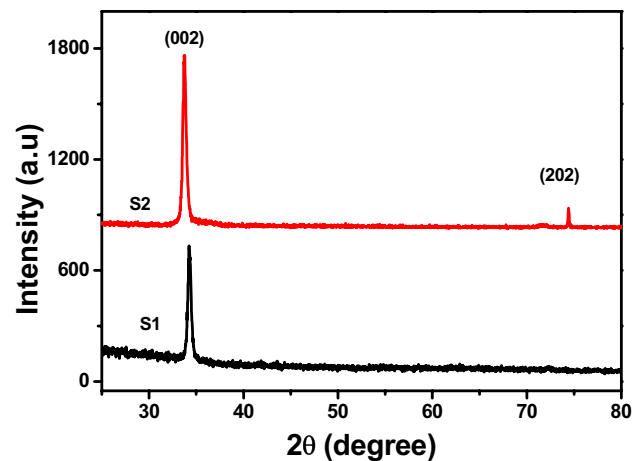
The lattice spacing can be calculated from Bragg's formula (Eq. 1)

$$2d\ \sin\theta\ =\ n\lambda \tag{1}$$

where d is the lattice spacing, θ is Bragg's diffraction angle, λ is wavelength and n is diffraction order (n = 1, 2, 3, 4…..).

ZnO crystallites have a hexagonal wurtzite structure. The lattice parameters 'a' and 'c' can be calculated from the following Eq. (2).

$$\frac{1}{d^2} = \frac{4}{3}\left(\frac{h^2 + hk + l^2}{a^2}\right) + \frac{l^2}{c^2} \tag{2}$$

where h, k, l are Miller indices, d is interplanar distance and 'a' and 'c' are lattice parameters.

The grain size along the c-axis has been calculated from Scherrer's formula Eq. (3)

$$D = \frac{K\lambda}{\beta\ cos\theta} \tag{3}$$

where K is constant, λ is the wavelength of value 0.154 nm, θ is Bragg's angle and β is full-width half maxima.

To examine the surface morphology, the prepared ZnO films were examined by field emission scanning electron microscope (FESEM, JEOL-JSM 6100) as shown in Fig. 4. It is observed that ZnO films for S1 (300 s) have not shown appreciable grains. Improvement in grain growth has been observed for S2 (800 s). The grain size of ZnO films has

Table 1 Structural parameter of ZnO films for S1 and S2 respectively

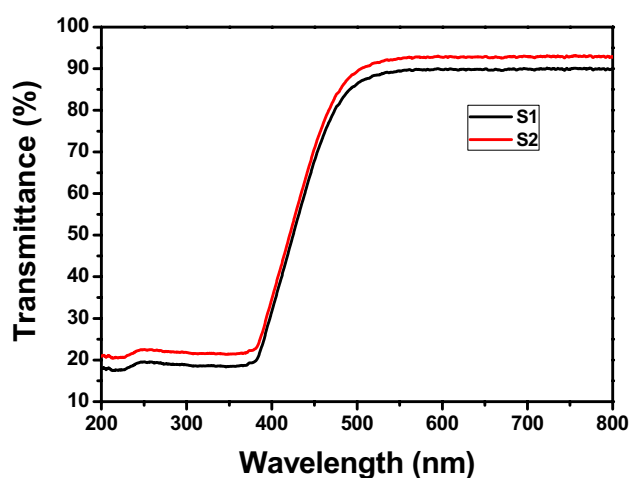| Sample	(hkl)	2θ (°)	Lattice parameters (Å)		Volume (Å)³	D (nm)	Thickness (nm)
			a	c			
S1	(002)	34.7	3.252	5.204	47.66	21	130
S2	(002)	34.3	3.258	5.209	47.88	17	170
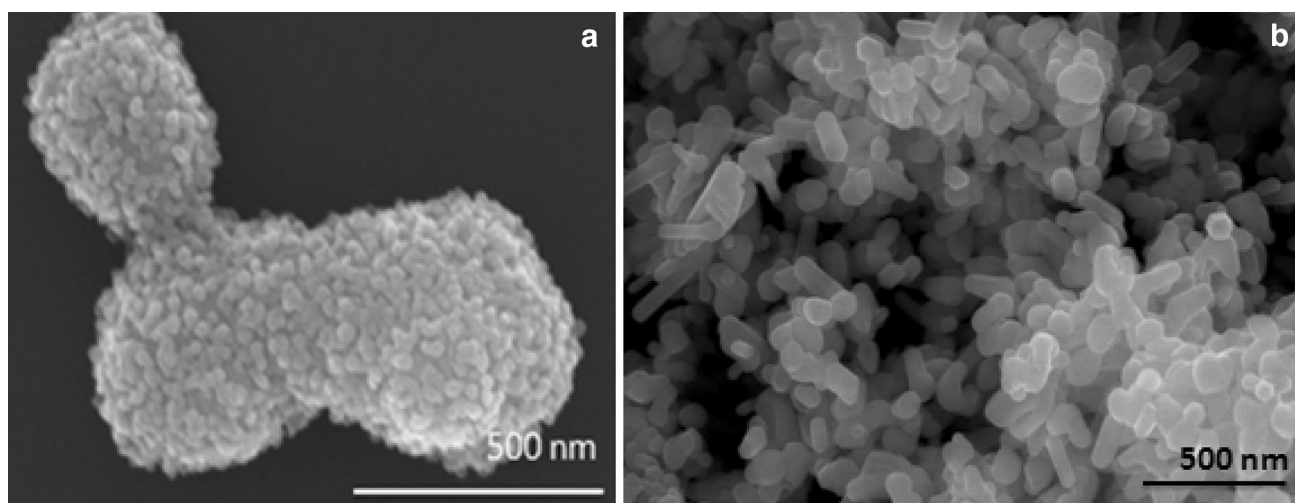
Fig. 4 a, b FESEM images of ZnO films for different deposition time (300 s, 800 s)
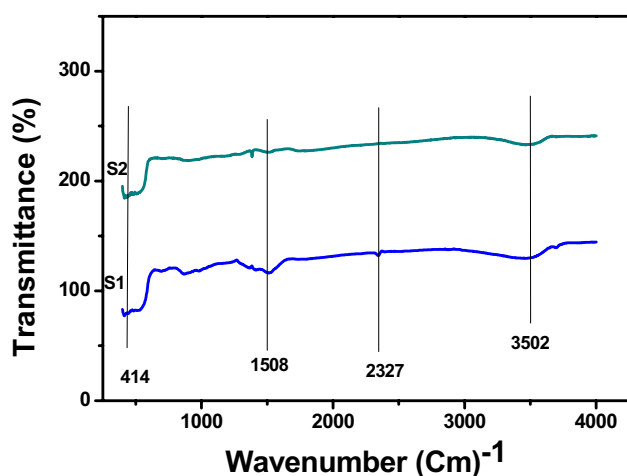
Fig. 5 FTIR spectra of ZnO films by varying deposition time

Fig. 6 UV–Vis spectra of ZnO films by varying deposition time (300 s, 800 s) respectively

increased from 80 to 120 nm. This increase in grain size indicates films are composed of less dense grain packing, revealing good quality. Sample S1 (300 s) exhibited smaller size nanorods. When the thickness of the films increased to 800 s (S2), the shape of nanorods becomes clear. This variation in morphology helps for better gas sensing response [21, 26]. It is also supported by XRD analysis that crystal size increases with the increase of deposition time.

Figure 5 shows the FTIR spectra as a function of a wavelength range from 4000 to 400 cm^{-1} by varying the deposition time. This spectrum predicts the ZnO stretching mode by showing a peak near 414 cm^{-1} [9, 21]. Another peaks near 1508 cm^{-1}, 2327 cm^{-1} and 3502 cm^{-1} corresponds to C=C, O=C=O and O=H bonds respectively [17, 25]. The film deposited for a low deposition time of 300 s contained full width at half maxima was 12.4 cm^{-1}. As the deposition

time is increased to 800 s, the full-width half maxima of the observed band are decreased to 5.6 cm^{-1} which are due to the improvement in crystallinity as observed in the XRD data.

In general, for the optoelectronic applications of ZnO, the highest value of transmittance is prerequisite. Figure 6 shows the wavelength versus transmittance of the ZnO films taken in the wavelength range from 200 to 800 nm. It has been observed that the transmittance (%) is increased with increase in deposition time from 300 s and 800 s. The variation in optical transmittance of the film in the visible region corresponds to change in crystalline quality and surface morphology [29]. Highest surface roughness leads to more surface scattering of light. Among different deposition time, deposited films for 800 s (S2) shows higher transmittance

than S1 (deposition time 300 s) which corresponds to the good crystalline quality of the films.

The optical absorption coefficient (α) was calculated from the film thickness and the optical transmittance data by using the relation (Eq. 4)
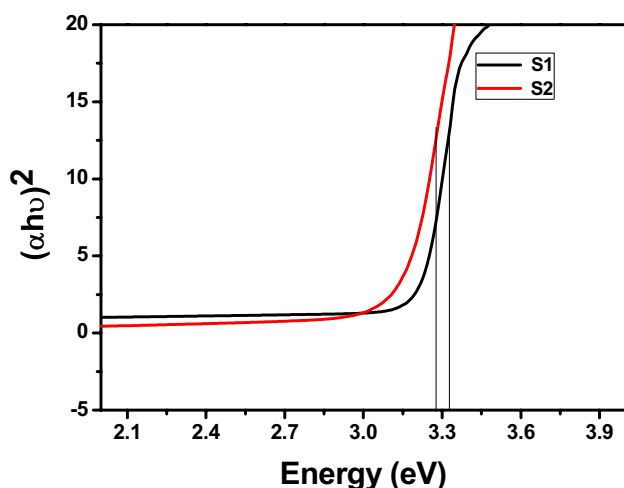
$$\alpha = (1/t)\,\ln T \tag{4}$$

Based upon the absorbance spectra, optical band gap E_g can be found by extrapolating linear portion of the plot $(\alpha h\nu)^2$ versus $h\nu$ for direct band gap. The absorbance coefficient for direct transition semiconductor is related to the optical band gap (E_g) according to following Eq. (5)

$$\alpha h\nu = A(h\nu - Eg)^{1/2} \tag{5}$$

where $h\nu$ is photon energy, E_g is the optical band gap, A is constant.

Figure 7 shows $(\alpha h\nu)^2$ plotted as a function of photon energy (eV) for ZnO. The extrapolation of a straight line to $\alpha h\nu = 0$ gives the value of direct optical band gap. Herein, bandgap decreased with increase in film thickness. This attributes to the variation in stress and lattice defects [30]. The wide band gap is expected to provide compressed lattice because of the increased repulsion between the oxygen 2p and the zinc 4 s bands. The value of transmittance and optical band gap are given in Table 2. Ning et al. demonstrates the self-power UV photodetector by aligning pure ZnO and Ag-doped ZnO nanofibers. This UV detector is found to have an enhanced performance, with the on–off ratio up to 104 at zero bias and a rather short rise/decay time of 3.90 s/4.71 s [27]. The decrease in bandgap is helpful for better optoelectronic applications [31–33].

Photoluminescence spectra (FP-6200, spectrofluorometer) is an effective way to study the optical properties of ZnO which is further helpful to find better gas sensing property.

Table 2 Optical study of ZnO films for different deposition time

Sample	Transmittance (%)	Band gap (eV)
S1	88	3.31
S2	90	3.29

Figure 8 shows PL spectra of ZnO thin films by varying deposition time. This characterization technique is performed at an excitation wavelength of 320 nm. Generally, ZnO has four PL emissions.

a) UV emission corresponds to a wavelength of 380 nm which attributes to free exciton recombinations.
b) An emission (blue and green) at 460 nm and 540 nm is due to intrinsic defects such as Zn interstitial and oxygen vacancies.
c) Green emission at 630 nm is due to the recombination of delocalized electrons with holes in oxygen interstitial.

Figure 8 shows in the visible region, broad peaks were observed near 407 nm and sharp emission was observed at 599 nm. These bands in the visible region have been attributed to recombination of photogenerated holes with intrinsic defects such as Zn interstitial and oxygen vacancies. More PL intensity has been observed in case of S2 which indicates more surface oxygen vacancies in case of S2 in comparison of S1. In addition to this, a sharp and broad peaks shift towards higher wavelength which may be due to the presence of defects and difference in the bandgap. This confirms that the structural, morphological and optical properties in conjunction with PL spectra enhance the defect concentration and reduce the crystallization which is the pre-requisites for gas sensing applications.

Fig. 7 Optical band gap calculations from Tauc's formula S1 and S2 respectively
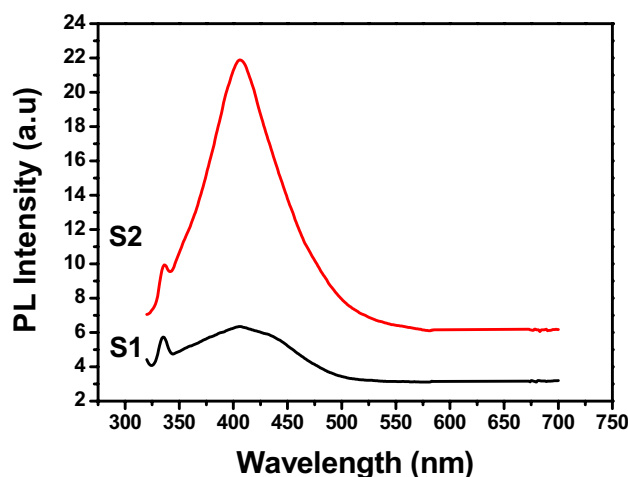
Fig. 8 Photoluminescence spectra of ZnO films by varying deposition time (*S1*, *S2*) respectively
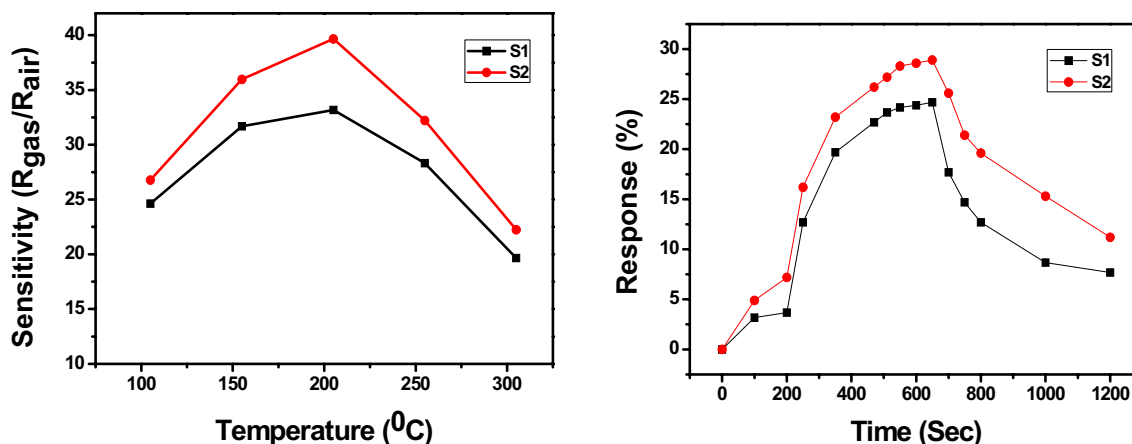
Fig. 9 Sensitivity and response characteristics for ZnO based sensor towards NO_2 gas

Figure 9 represents temperature-dependent sensitivities against NO_2 gas. All the synthesized films show 205 °C is an optimum temperature. Beyond this temperature sensitivity of all the samples is decreased which may be due to a lesser extent of adsorption of O_2 and nitrogen molecules on the surface of sensor materials. This figure shows the sensitivity of ZnO films towards NO_2 at different operating temperature. Figure 9 reveals the sensitivity of the synthesized samples and it has found that the increase in gas sensing response may be due to improvement in crystallinity and surface to volume ratio. This is responsible for the reduction in electron–hole pair recombination [34]. The sensitivity of the sensor is increased up to 205 °C and thereafter it decreases. This is due to the fact that at low temperature, a low response of the sensor is observed because the gas molecules do not have enough thermal energy to react with adsorbed oxygen species. Figure 9 also demonstrates the response at 3 vol% of NO_2 gas concentration was 23.7% and 28.3% respectively. The increasing sensitivity has a positive relationship with deposition time. This result also has a positive correlation with XRD, FESEM and UV–Vis spectroscopy. Therefore optimum deposition time is 800 s yields to maximum sensitivity.
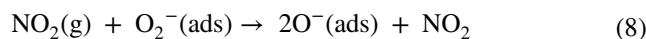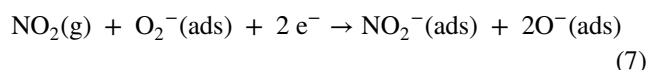
3.2 Gas sensing mechanism

The proposed mechanism for gas sensing application has been introduced. Absorbed gas plays an important role to change the electrical resistance. When the synthesized samples exposed to air, it absorbs the oxygen molecules and forms different ionic species O^{n-} (O_2^-, O_2^{2-}, O^{2+}). These ions help to create the depletion layer on the host surface. These ionic species are responsible to enhance the sensitivity. Whereas, when the sensor is exposed to the donor (reducing gas) the electron trapped by oxygen adsorbate will return to ZnO films when leads to decrease in the potential barrier which increases the conductivity of the films.

Adsorption and desorption of test gas molecules are the main issues to understand the gas sensing mechanism. It forms the ionic species on the sample surface. It clearly shows that 800 s deposition time (S2) yields the best sensing response at 205 °C. As response and recovery time are important parameters for evaluating the sensor potential applications [27, 34]. The prepared films have quick response time 128 s and fast recovery time 163 s respectively. The sensing mechanism is also based on the principle of chemiresistance. Change in resistance of metal oxide film depends on the type of gas molecules and majority carriers. Typically, oxygen in air adsorbed on the surface of ZnO. These oxygen species can capture the electron from the surface of ZnO films and form oxygen species. These oxygen species helps to create the depletion layer on the host surface and thus reduce conductivity [35]. Whereas, when the sensor is exposed to reducing gas the electron is trapped by the oxygen adsorbate will return to ZnO film which leads to a decrease in the potential barrier and increases the conductivity. It helps for better gas sensing response.

When the sensor films are exposed to oxidizing gas (NO_2), these molecules are directly adsorbed on to the surface (Eq. 6) and they can be the part of chemisorbed oxygen Eqs. (7, 8)

$$NO_2(g) + e^- \rightarrow NO_2^- \tag{6}$$

$$NO_2(g) + O_2^-(ads) + 2e^- \rightarrow NO_2^-(ads) + 2O^-(ads) \tag{7}$$

$$NO_2(g) + O_2^-(ads) \rightarrow 2O^-(ads) + NO_2 \tag{8}$$

These equations confirm the interesting role of adsorption of O_2^- ions. Hence as synthesized ZnO films can act as very efficient gas sensors for various poisonous gases. This mechanism illustrates more oxygen to be adsorbed and

increased the surface area which is responsible to enhance the response.

4 Conclusions

To conclude ZnO films were synthesized by facile and rapid rf magnetron sputtering method. Detailed characterizations confirmed that variation in deposition time exhibited good optoelectronic properties. Gas sensing property confirms that response of ZnO films has been increased with an increase in deposition time. Nanorods shaped morphology exhibits better gas sensing response than the films prepared on less deposition time. Herein, 205 °C is considered to be optimum temperature. The prepared films are found to have quick response time 128 s and fast recovery time 163 s. Hence as-synthesized ZnO films can be used for the fabrication of nanodevice which is further used for gas sensing properties to detect various poisonous gases.

References

1. G. Singh, S.B. Shrivastava, D. Jain et al., Effect of indium doping on zinc oxide films prepared by chemical spray pyrolysis technique. Bull. Mater. Sci. **33**, 581–587 (2011). https://doi.org/10.1007/s12034-010-0089-6
2. Y.I. Alivov, Fabrication and characterization of n -ZnO Õ p-AlGaN heterojunction light-emitting diodes on 6H-SiC substrates. Appl. Phys. Lett. **83**, 4719–4721 (2003). https://doi.org/10.1063/1.1632537
3. R. Pietruszka, B.S. Witkowski, S. Gieraltowska et al., New efficient solar cell structures based on zinc oxide nanorods. Sol. Energy Mater. Sol. Cells **143**, 99–104 (2015). https://doi.org/10.1016/j.solmat.2015.06.042
4. F. Teng, L. Zheng, K. Hu, H. Chen, Y. Li, Z. Zhang, X. Fang, A surface oxide thin layer of copper nanowires enhanced the UV selective response of a ZnO film photodetector. J. Mater. Chem. C **4**, 8416–8421 (2016). https://doi.org/10.1039/C6TC02901A
5. H. Lin, S.M. Zhou, J.H. Zhou et al., Structural and optical properties of a-plane ZnO thin films synthesized on gamma-LiAlO(2) (302) substrates by low-pressure metal-organic chemical vapor deposition. Thin Solid Films **516**, 6079–6082 (2008). https://doi.org/10.1016/j.tsf.2007.10.128
6. S. Bhatia, N. Verma, A. Mahajan, R.K. Bedi, Characterization of ZnO films based sensors prepared by different techniques. Appl. Mech. Mater. **772**, 50–54 (2015). https://doi.org/10.4028/www.scientific.net/AMM.772.50
7. W.-J. Chen, W.-L. Liu, S.-H. Hsieh, Y.-G. Hsu, Synthesis of ZnO:Al transparent conductive thin films using sol-gel method. Procedia Eng. **36**, 54–61 (2012). https://doi.org/10.1016/j.proeng.2012.03.010
8. N.V. Kaneva, C.D. Dushkin, Preparation of nanocrystalline thin films of ZnO by sol-gel dip coating. Bulg. Chem. Commun. **43**, 259–263 (2011)
9. S. Bhatia, N. Verma, R.K. Bedi, Optical application of Er-doped ZnO nanoparticles for photodegradation of direct red-31 dye. Opt. Mater. **62**, 392–398 (2016). https://doi.org/10.1016/j.optmat.2016.10.013
10. N. Srinatha, Y.S. No, V.B. Kamble et al., Effect of RF power on the structural, optical and gas sensing properties of RF-sputtered Al doped ZnO thin films. RSC Adv **6**, 9779–9788 (2016). https://doi.org/10.1039/C5RA22795J
11. L. Saikia, D. Bhuyan, M. Saikia, B. Malakar, D.K. Dutta, P. Sengupta, Photocatalytic performance of ZnO nanomaterials for self sensitized degradation of malachite green dye under solar light. Appl. Catal. A Gen. **490**, 42–49 (2015). https://doi.org/10.1016/j.apcata.2014.10.053
12. N. Nafarizal, Precise control of metal oxide thin films deposition in magnetron sputtering plasmas for high performance sensing device fabrication. Procedia Chem. **20**, 93–97 (2016). https://doi.org/10.1016/j.proche.2016.07.016
13. M. Dwivedi, A. Bhargava, A. Sharma, V. Vyas, G. Eranan, CO sensor using ZnO thin film derived by RF magnetron sputtering technique. IEEE Sens. **14**, 1577–1582 (2014). https://doi.org/10.1109/JSEN.2014.2298879
14. X. Peng, Z. Wang, Y. Song et al., Structural and photoluminescent properties of ZnO films deposited by radio frequency reactive sputtering. Sci. China Ser. G: Phys. Mech. Astron. **50**, 281–286 (2007). https://doi.org/10.1007/s11433-007-0007-0
15. R.O. Ndong, H.M. Omanda, P. Soulounganga, Effect of target to substrate distance on the rf magnetron sputtered ZnO thin films. Int. J. Mater. Sci. **17**, 122–126 (2013)
16. M. Becerril, H. Silva-López, A. Guillén-Cervantes, O. Zelaya-Ángel, Aluminum-doped ZnO polycrystalline films prepared by co-sputtering of a ZnO-Al target. Rev. Mex. Fis. **60**, 27–31 (2014)
17. J.-W. Hoon, K.-Y. Chan, J. Krishnasamy, T.-Y. Tou, Zinc oxide thin films fabricated with direct current magnetron sputtering deposition technique. Physics **1328**, 235–237 (2011). https://doi.org/10.1063/1.3573740
18. S. Bhatia, N. Verma, R.K. Bedi, Applied Surface Science Sn-doped ZnO nanopetal networks for efficient photocatalytic degradation of dye and gas sensing applications. Appl. Surf. Sci. **407**, 495–502 (2017). https://doi.org/10.1016/j.apsusc.2017.02.205
19. X. Fang, L. Hu, C. Ye, L. Zhang, One-dimensional inorganic semiconductor nanostructures: a new carrier for nanosensors. Pure Appl. Chem. **82**, 2185–2198 (2010)
20. V. Kumar, V. Kumar, S. Som et al., Effect of annealing on the structural, morphological and photoluminescence properties of ZnO thin films prepared by spin coating. J. Colloid Interface Sci. **428**, 8–15 (2014). https://doi.org/10.1016/j.jcis.2014.04.035
21. S. Bhatia, N. Verma, R.K. Bedi, Varied sensing characteristics of in- doped ZnO films prepared by sol gel spin coating technique. Indian J Pure Appl Phys **13**, 54–58 (2017)
22. N.K. Ponon, D.J.R. Appleby, E. Arac et al., Effect of deposition conditions and post deposition anneal on reactively sputtered titanium nitride thin films. Thin Solid Films **578**, 31–37 (2015). https://doi.org/10.1016/j.tsf.2015.02.009
23. A. Taabouche, A. Bouabellou, F. Kermiche et al., Effect of substrates on the properties of ZnO thin films grown by pulsed laser deposition. Adv. Mater. Phys. Chem. **3**, 209–213 (2013). https://doi.org/10.4236/ampc.2013.34031
24. S. Bhatia, N. Verma, R.K. Bedi, Effect of aging time on gas sensing properties and photocatalytic efficiency of dye on in-Sn co-doped ZnO nanoparticles. Mater. Res. Bull. (2016). https://doi.org/10.1016/j.materresbull.2016.12.011

25. S. Bhatia, N. Verma, R.K. Bedi, Ethanol gas sensor based upon ZnO nanoparticles prepared by different techniques. Results Phys. (2017). https://doi.org/10.1016/j.rinp.2017.02.008

26. S. Bensmaine, B. Benyoucef, Effect of the temperature on ZnO thin films deposited by r.f. magnetron. Phys. Procedia. **55**, 144–149 (2014). https://doi.org/10.1016/j.phpro.2014.07.021

27. G.S. Hikku, R.K. sharma, R.V. William, P. Thiruramanathan, Al-Sn doped ZnO thin film nanosensor for monitoring NO_2 concentration. J. Taibah Univ. Sci. (2016). https://doi.org/10.1016/j.jtusci.2016.02.002

28. S. Bhatia, N. Verma, R. Kumar, Morphologically-dependent photocatalytic and gas sensing application of Dy-doped ZnO nanoparticles. J. Alloy Compd. **726**, 1274–1285 (2017). https://doi.org/10.1016/j.jallcom.2017.08.048

29. B. Yuliarto, S. Julia, M. Iqbal, M.F. Ramadhani, N. Nugraha, et al (2015) The effect of tin addition to ZnO nanosheet thin films for ethanol and isopropyl alcohol sensor applications. J. Eng. Technol. Sci. 47:76–91. https://doi.org/10.5614/j.eng.technol.sci.2015.47.1.6

30. R.S. Reddy, A. Sreedhar, A.S. Reddy, S. Uthanna, Effect of film thickness on the structural morphological and optical properties of nanocrystalline ZnO films formed by RF magnetron sputtering. Adv. Mater. Lett. **3**, 239–245 (2012). https://doi.org/10.5185/amlett.2012.3329

31. D.S. Dhawale, D.P. Dubal, A.M. More et al., Room temperature liquefied petroleum gas (LPG) sensor. Sens. Actuators B: Chem. **147**, 488–494 (2010). https://doi.org/10.1016/j.snb.2010.02.063

32. N.C. Net, E. Engineering, U. Teknologi et al., (2015) Study on doping effect of Sn doped ZnO thin films for gas sensing application. In IEEE Student Conference on Research and Development, pp. 435–440

33. B. Radha, R. Rathi. K.C. Lalithambika, A. Thayumanavan, K. Ravichandran. S. Sriram, Effect of Fe doping on the photocatalytic activity of ZnO nanoparticles: experimental and theoretical investigations. J. Mater. Sci.: Mater. Electron. **29**, 13474–13482 (2018)

34. Y. Ning, Z. Zhnag, F. Teng, X. Fang (2018) Novel transparent and self-powered UV photodetector based on crossed ZnO nanofiber array homojunction. Small **14**, 1703754, https://doi.org/10.1002/smll.201703754

35. S. Bhatia, R.K. Bedi, Morphological, electrical and optical properties of zinc oxide films grown on different substrates by spray pyrolysis technique. Nanostruct. Thin Films III **7766**, 776610–776610 (2010). https://doi.org/10.1117/12.863878